HYDROLOGICAL PROCESSES
*Hydrol. Process.* (2014)
Published online in Wiley Online Library
(wileyonlinelibrary.com) DOI: 10.1002/hyp.10141

# Hydrologic response to valley-scale structure in alpine headwaters

Anne A. Weekes,[1,2]* Christian E. Torgersen,[2] David R. Montgomery,[3] Andrea Woodward[4] and Susan M. Bolton[1]

[1] *College of the Environment, School of Environmental and Forest Sciences, University of Washington, Box 352100, Seattle, WA 98195-2100, USA*
[2] *US Geological Survey, Forest and Rangeland Ecosystem Science Center, Cascadia Field Station, University of Washington, Box 352100, Seattle, WA 98195-2100, USA*
[3] *Department of Earth and Space Sciences, Quaternary Research Center, University of Washington, Box 351310, Seattle, WA 98195, USA*
[4] *US Geological Survey, Forest and Rangeland Ecosystem Science Center, Olympic Field Station, Port Angeles, WA 98362, USA*

## ABSTRACT:

Few systematic studies of valley-scale geomorphic drivers of streamflow regimes in complex alpine headwaters have compared response between catchments. As a result, little guidance is available for regional-scale hydrological research and monitoring efforts that include assessments of ecosystem function. Physical parameters such as slope, elevation range, drainage area and bedrock geology are often used to stratify differences in streamflow response between sampling sites within an ecoregion. However, these metrics do not take into account geomorphic controls on streamflow specific to glaciated mountain headwaters. The coarse-grained nature of depositional features in alpine catchments suggests that these landforms have little water storage capacity because hillslope runoff moves rapidly just beneath the rock mantle before emerging in fluvial networks. However, recent studies show that a range of depositional features, including talus slopes, protalus ramparts and 'rock-ice' features may have more storage capacity than previously thought.

To better evaluate potential differences in streamflow response among basins with extensive coarse depositional features and those without, we examined the relationships between streamflow discharge, stable isotopes, water temperature and the amplitude of the diurnal signal at five basin outlets. We also quantified the percentages of colluvial channel length measured along the stepped longitudinal profile. Colluvial channels, characterized by the presence of surficial, coarse-grained depositional features, presented sediment-rich, transport-limited morphologies that appeared to have a cumulative effect on the timing and volume of flow downstream. Measurements taken from colluvial channels flowing through depositional landforms showed median recession constants ($K_r$) of 0.9–0.95, $\delta^{18}O$ values of $\geq -14.5$ and summer diurnal amplitudes $\leq 0.8$ as compared with more typical surface water recession constant values of 0.7, $\delta^{18}O \leq -13.5$ and diurnal amplitudes $>2.0$. Our results demonstrated strong associations between the percentage of colluvial channel length within a catchment and moderated streamflow regimes, water temperatures, diurnal signals and depleted $\delta^{18}O$ related to groundwater influx. Copyright © 2014 John Wiley & Sons, Ltd.

KEY WORDS colluvial channels; groundwater; talus slopes; alpine headwaters

*Received 20 September 2011; Accepted 22 December 2013*

## INTRODUCTION

Understanding streamflow regimes – the timing, magnitude and duration of flow that drive aquatic habitat function in glaciated mountain headwaters – is complicated by the spatial and temporal complexity of geohydrologic processes in such terrains. Insight into hydrologic response associated with diverse source waters as well as the physicochemical properties of these waters is of fundamental importance for ecological monitoring and research (Milner and Petts, 1994; Ward, 1994; Brown *et al*., 2003; Brown *et al*., 2006; Brown *et al*., 2007; Brown *et al*., 2009). The spatial and temporal complexity of hydrologic response is due to many factors caused by heterogeneous mountain terrain (i.e. differences in topography, elevation, geomorphic and geologic materials, structures and processes at multiple scales). These conditions present a challenge to understanding ecosystem function, particularly at larger scales.

The mechanisms that drive patterns of hydrologic response at the basin scale in alpine headwaters (i.e. $\leq 20$ km) are difficult to model using small-scale physics (e.g. coupled balance equations for mass and momentum)

*Correspondence to: Anne A. Weekes, College of the Environment, School of Environmental and Forest Resources, University of Washington, Box 352100, Seattle, WA 98195-2100, USA.
E-mail: aaw2@uw.edu

and theories such as Darcy's law and the Richards equation (McDonnell *et al.*, 2007). Particularly for ecological applications in heterogeneous terrain, it may not be useful to 'scale up' or extrapolate from small-scale physical parameters to account for the disproportionate importance of specific intermediate-scale (i.e. valley segment-scale to valley-scale) controls on streamflow response (Frissell *et al.*, 1986; Klemes 1988; Poff, 1997; Downes, 2010). Understanding the causal mechanisms that drive streamflow in complex topographies at larger scales requires tools to differentiate between suites of linked geomorphic elements associated with particular streamflow regimes that may exhibit emergent properties and functional traits.

The longitudinal profile drives the local and systematic downstream spatial organization of geomorphic processes that are associated with streamflow response within the channel network (Brardinoni and Hassan, 2006; Collins and Montgomery, 2011). In many glaciated mountain landscapes, the stepped longitudinal profile provides a common structural framework composed of heterogeneous paraglacial landforms (i.e. talus slopes and other depositional landforms produced by deglaciation and post-glacial mass wasting processes) and glacial macroform structures (e.g. cirque and hanging glacial valleys, bedrock canyons, glacial moraines and rock glacier deposits) that determine the sequence of channel types and differences in water storage, runoff and exfiltration mechanisms (Figure 1) (Brardinoni and Hassan, 2006).

Differences in post-glacial landforms produced by diverse mass wasting processes have many hydrologic properties; many of these landforms originate from antecedent climate regimes (Clow *et al.*, 2003; Brardinoni and Hassan, 2006). For example, in the Sierra Nevada (USA), researchers have identified six classes of post-glacial 'rock-ice' features that demonstrate different water storage and exfiltration mechanisms beyond serving as conduits for runoff (Millar and Westfall, 2008). Intermediate-scale landforms act as filters that influence runoff and affect snowmelt and ice melt processes to produce diverse and spatially variable groundwater, surface and subsurface flows.

Like lowland stream networks, the landforms that constitute the stream and its valley contribute to a spatial mosaic of independent temporal filters (i.e. features that affect the timing of flows within a channel as well as those released from melting ice lenses and groundwater reservoirs) at multiple scales. Each subarea within a drainage basin develops processes that respond differently to water and energy inputs and are linked to one another by the valley structure or stream network (Woods, 2002). In more complex alpine topography, a variety of channel types at valley segment and reach scales are embedded within multiple geomorphic contexts that affect the mechanisms that filter and route streamflow.

We hypothesized that differences in channel morphology and process at valley-scale and valley segment-scale along the channel longitudinal profile would, in aggregate, influence downstream flow regimes. We ask whether these valley-scale and valley segment-scale morphologies correspond with process domains (*sensu* Montgomery, 1999) produced by fluvial and post-glacial processes and mass movements that constitute geohydrologic elements with common functional traits.

Our first objective was to test the usefulness of colluvial, alluvial and bedrock channel types associated with differences in channel transport capacity and sediment supply characteristics that may drive variability in hydrologic patterns (e.g. runoff and storage) (Swanson *et al.*, 1988; Montgomery and Buffington, 1997; Brardinoni and Hassan, 2006; Weekes *et al.*, 2012). Using hydrologic indices (i.e. recession constants, stable isotope analysis and water temperature) and channel classification, we evaluated streamflow discharge characteristics from five headwater catchments in Mount Rainier National Park (MORA) (USA) over a 3-year period. Such understanding may improve our ability to assess and model macroscale differences among basin-wide streamflow responses across mountain regions.

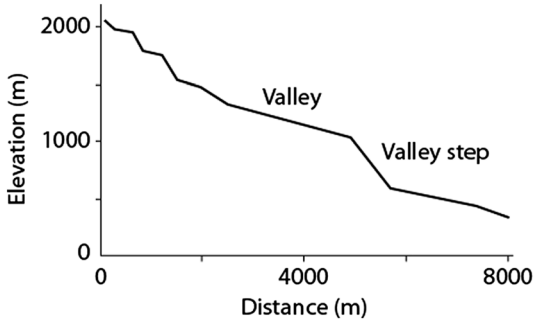


Figure 1. Schematic of stepped channel longitudinal profile in relict glaciated mountain headwaters with typical valley and valley step morphology

## SITE DESCRIPTION

The study area is located within Mount Rainier National Park (MORA), which encompasses 954 $km^2$ surrounding a 4392-m glaciated volcano on the west side of the Cascade Range in Washington State, USA. We selected five headwater catchments located in hard metamorphic rocks that predate the volcano, which were shaped most recently by erosion and deposition from minor Holocene alpine glaciers. The upper basins of Crystal, Deer and Lost Creeks hold relict rock glacier deposits that may have been active until very recently (i.e. through the end

of the Little Ice Age, ca 1830). Glaciation at MORA was not affected by the Cordilleran Ice Sheet during the Pleistocene. All five study basins were covered by alpine glaciers, but the upper basin summits were ice-free (Crandell, 1969; Tsukada *et al*., 1981).

The study sites were located on the east side of Mount Rainier (Figure 2) with a slightly drier average climate than the west side of the volcano. All basins have similar elevational variation (mean: 1090 m; range of mean elevation: 165 m) and comparable mean channel slope (11–17%). Laughingwater Creek is slightly lower in elevation overall (Table I). Headwater drainage areas vary from 4–15 km$^2$; however, Crystal Creek's drainage area is >3× smaller than Lost, Deer and Laughingwater, and 6% steeper than the other basins. Four USDA SNOTEL sites at elevations ranging from 900–1800 m surround the MORA study sites provided climate data at a subregional scale. All SNOTEL stations, including Morse Lake, Cayuse Pass, Corral Pass and Huckleberry were located within 6 miles of the study sites. The dominant wind direction is from the southwest and west off the Pacific Ocean.

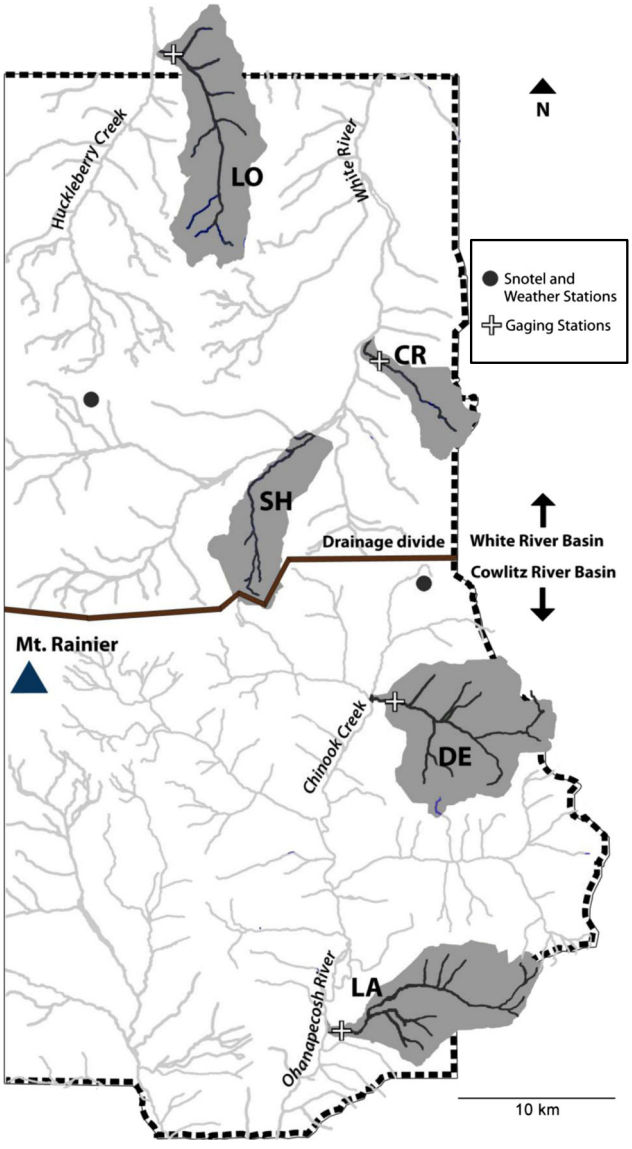


Figure 2. Locations of Lost (LO), Crystal (CR), Shaw (SH), Deer (DE) and Laughingwater (LA) Creeks, relict glacial headwaters on the east side of Mount Rainier National Park, Washington state, USA. The park boundary (heavy dashed line) is shown for the northeast and southeast quadrants of the park

The winter hydrology of the five basins is currently snow dominated with the exception of Laughingwater Creek; over half of the basin is below 1200 m, the mean freezing level for Mount Rainier National Park during the period 1948–2013 (http://www.wrcc.dri.edu/cwd). Most precipitation falls as snow or rain on snow (ROS) between November and February. However, atmospheric rivers (ARs), frontal low-pressure systems from the Pacific Ocean, cause a rise in the elevation of the ROS zone, rising as high as 2438 m during some storms (Neiman *et al*. 2011; Ralph and Dettinger 2011). The plume of maximum saturation striking the Cascades front occurs around 900 m; lower elevations exhibited less rainfall. Because of the fall and winter occurrence of most AR events, intense rainfall produced by ARs often falls on antecedent snow cover, although the effects of intense rain melting antecedent snow may be secondary compared with the rainfall intensity characteristic of some AR storms (Neiman *et al*. 2011; Ralph and Dettinger 2011). Regardless, ARs have been the cause of the largest regional flood events in the past 25 years and are associated with an increased incidence of mass movements in steep terrain.

## METHODS

### *Hydrogeomorphic characterization*

The glacial macroforms that make up the stepped longitudinal profile found in the study basins were identified using standard methods including air photo interpretation, geographic information system based topographic analysis and field surveys. Aerial photos flown in 1984 and 2002 were scanned into ArcGIS 9.3 (Esri, Redlands, CA) and manipulated to develop stereoscopic 3D images of the basins using the ESRI 3D analyst extension with ArcScene. Additional map layers included flow direction and flow accumulation grids based on 10-m resolution digital elevation models, and the MORA map of surficial geology (Crandell, 1969).

Using map overlays in geographic information system, we delineated a preliminary version of the channel longitudinal profile and identified structures such as talus slopes, relict rock glacier deposits and landslides within

Table I. Drainage area, mean channel slope, maximum and minimum basin elevation, and mean channel elevation for headwater drainage basins in Mount Rainier National Park.

| Stream/ subwatershed | Major watershed | Drainage area (km2) | Mean slope (channel) % | Maximum elevation (basin) (m) | Minimum elevation (basin) (m) | Mean elevation (channel) (m) |
|---|---|---|---|---|---|---|
| Crystal | White | 4.1 | 17.0 | 2129 | 949 | 1434 |
| Lost | White | 14.0 | 11.0 | 2136 | 975 | 1456 |
| Shaw | White | 8.2 | 11.0 | 2063 | 1026 | 1426 |
| Deer | Cowlitz | 14.5 | 11.0 | 2010 | 887 | 1423 |
| Laughingwater | Cowlitz | 14.2 | 12.0 | 1697 | 591 | 1038 |

each study catchment, ranging in size from 100 to 1 ha. Finer-scale features found within each step along the longitudinal profile were assessed visually in the field to evaluate the linkage between landform and channel. Field surveys of channel cross sections and the longitudinal profiles were used to demarcate the break in slope between valley floors and valley steps and identify connections between channel and hillslope features.

The spatial extent of alpine headwater basins was small; unlike lowland river classification schemes that generally differentiate between channel morphology and process characteristics at the reach-scale (EMAP), the differences that we found in channel type varied synchronistically with the adjoining valley or valley step because of the constraints caused by glacial macroform structures. Therefore, the valley segment-scale or valley-scale generally matched differences in channel morphology along the longitudinal profile. Channel types were identified following the process-based categories (i.e. colluvial, alluvial and bedrock) developed by Montgomery and Buffington (1997) for unglaciated mountain basins and subdivided into source and sink colluvial channels based on categories developed by Brardinoni and Hassan (2006; 2007) for relict glaciated headwaters.

Valley types were assessed using standard geomorphic field techniques (Grant *et al.*, 1990) and subdivided into source and sink colluvial, alluvial and bedrock categories (Montgomery and Buffington, 1997; Brardinoni and Hassan, 2007). Contrary to basins dominated by fluvial processes in unglaciated mountain drainage areas, colluvial channels represented a transport-limited and sediment-rich endpoint on the continuum of streamflow dynamics characterized by $Q_c < Q_s$, where $Q_c$ represents transport capacity and $Q_s$ represents sediment supply (Figure 3). Source colluvial valleys produced channels with subsurface flows within depositional landforms in the upper basin, whereas sink colluvial channels had buried channels or underfit surface channels with subsurface flows associated with debris flows, landslides and other disturbance features. In hydrologic terms, these channels differ functionally; source channels are associated with exfiltration of source waters in the channels initiation zone. Sink channels are infiltrated by alluvial and bedrock channel flow from upstream. Bedrock channels and canyons were supply limited ($Q_c > Q_s$) and thus represented the opposite extreme. Cascade, step-pool and other alluvial channel morphologies, classified as alluvial valleys, were characterized by intermediate transport capacity and sediment supply relationships.

### *Recession constants*

Gaging stations located in the lower headwaters logged hourly data over a 3-year period from October 2004 through November 2006. Pressure transducers (Global Water W15, Gold River, CA) were located at channel cross sections with bedrock control in Crystal, Deer and Laughingwater Creeks. The Shaw Creek channel was buried by a recent debris flow and could not be gaged. However, this creek is an important example of colluvial channel processes and morphology. For Lost Creek, we selected a stable location with comparatively regular channel geometry. Stage-discharge rating curves were developed for each gage site using standard techniques (Rantz, 1982) to generate streamflow discharge.

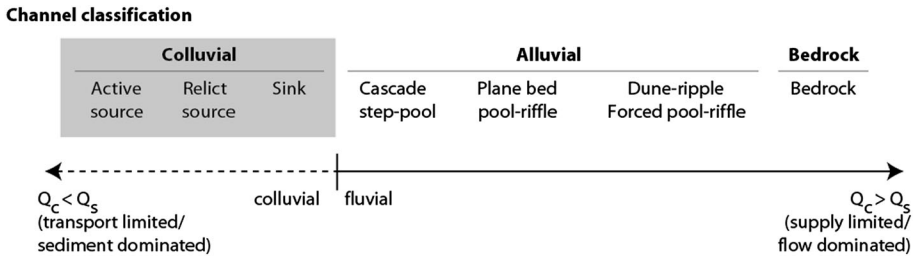


Figure 3. Continuum of alpine headwater channel characteristics that encompass the range of sediment supply and transport capacity relationships across the spectrum of ratios of transport capacity ($Q_c$) to supply ($Q_s$) often used for stream classification

Recession constants were used to quantify the falling limb of the stream hydrograph and were computed for all basins with the exception of Shaw Creek. We used the linearized Depuit-Boussinesq equation for the storm hydrograph (Tallaksen, 1995; Fetter, 2001; Montgomery and Dietrich, 2002)

$$Q_t = Q_p{}^{e-\alpha t} = Q_p K_r{}^t \quad (1)$$

where $Q_p$ is peak discharge at time $t = 0$ (hours), $Q_t$ is the flow at a later time $t$ and $K_r$ is a recession constant for the basin that is less than unity.

Comparative $K_r$ values generated by Montgomery and Dietrich (2002) for Oregon Coast Range headwaters for vadose zone processes in unglaciated mountain headwaters were used to interpret runoff mechanisms from the recession constants for the study basins. However, the filtering, storage and runoff effects produced by colluvial materials in glaciated headwaters involved hydrologic mechanisms that are poorly documented in the literature. Therefore, $K_r$ values were used for comparative purposes only; lower $K_r$ values are associated with faster flow pathways ($<0.69$) such as Hortonian overland flow, whereas higher values ($>0.88$) are associated with slower groundwater flowpaths (Montgomery and Dietrich, 2002).

*Stable isotope analysis*

We used stable isotope values in this study to compare and contrast the gross effect of colluvial channel morphology on the timing of the $\delta^{18}O$ discharge signature with those for alluvial channels. If channel geomorphology is an important contributing factor to channel routing and filtering mechanisms, these characteristics will contribute to the shape of the stream hydrograph and can be measured using common hydrologic indices used in baseflow residence time studies in soil-covered catchments. Stable isotope values have been used to calculate 'contact time', the residence time of water in soil using topographic and soils data (i.e. hydraulic conductivity, a storage coefficient and a mean watershed wetness index) (Wolock *et al.*, 1997). Subsequent work has shown that recession analysis can be used in place of environmental tracers to establish baseflow residence time at the watershed scale (Vitvar *et al.*, 2002). Therefore, we determined that the stable isotope signature among basins should correspond to the recession pattern. We assumed that runoff and water storage processes within the soil-mantled hillslopes were comparable between basins, so differences in both stable isotope and recession constants were a function of channel geomorphology.

We assessed potential differences in median $\delta^{18}O$ concentrations and seasonal patterns between five basins from June 2004 to November 2006. Grab samples were taken at downstream gage locations at different flow periods to assess potential seasonal differences (i.e. spring snowmelt [May–June], transition to baseflow [July], summer baseflow [August] and early fall baseflow [September]). Initially, we obtained three or more samples at half hour intervals at each gage site to check if values fluctuated. When it became apparent that values for each creek were consistent (standard error $\leq 1\%$), the number of samples was reduced to one or two samples per gage.

Stream basins volumetrically integrate differences in the stable isotope signature from parent atmospheric waters and phase changes at the ground surface that produce the ever-changing $\delta^{18}O$ signal of source waters. Research has shown extreme variation in $\delta^{18}O$ values in stream discharge and precipitation at many spatial ($km^2$ to $m^2$) and temporal scales (intra-seasonal variability to years) (Ingraham 1998). Fractionation of $\delta^{18}O$ enriches or depletes values as state changes between water vapour, liquid water and snow and ice. For example, compared with a basin mean, isotope values are depleted in freshly fallen snow, hail, occult precipitation and during refreezing of the snowpack and ice lenses; $\delta^{18}O$ is enriched during snowmelt and ice melt (Rodhe, 1998).

The $\delta^{18}O$ signal in precipitation is controlled by differences in atmospheric temperatures at the time of cloud formation that vary according to differences in season and elevation. The stable isotope signature is also dependent on the 'amount effect' associated with the intensity and duration of precipitation and spatial variability associated with the 'continental effect'. Seasonal differences appear to have the largest effect on $\delta^{18}O$, followed by elevation. Differences in air temperature at the time of cloud formation cause variation in precipitation $\delta^{18}O$ values. For example, values measured in 2005 at Cle Elum at 583 m elevation on the leeward side of the North Cascades range, varied 6.6 ‰ between winter and summer (Robertson and Gazis, 2006). The 'altitude effect' refers to the well-documented relationship between air temperature and elevation and is especially pronounced in high elevations and on the lee side of mountain ranges (Dansgaard, 1964).

The Burk and Stuiver equation (1981) was designed to model the 'altitude effect' specific to MORA, offering a generalized relationship between isotope values in precipitation and elevation to provide probable $\delta^{18}O$ values for recharge input (precipitation) using standard mean ocean water as a basis:

$$M = -313\cdots\delta^{18}O\text{–}2729 \quad (2)$$

where $M$ is the elevation in metres based on the measured $\delta^{18}O$ values for precipitation. The equation is in agreement with the mean temperature lapse rate on

Mount Rainier of 5.2 °C per 1000 m (Burk and Stuiver, 1981). We substituted the mean $\delta^{18}O$ output values from the study sites into the equation to see if the resulting modelled elevations matched the mean basin elevations derived from a LiDAR-generated digital elevation model that was validated with global positioning system field measurements (Table I). We used this equation to test if these stream basins were dominated by overland flow. If so, theoretically, the MORA headwaters should have $\delta^{18}O$ values that are related to those found in local precipitation (Criss, 1999).

The 'amount effect' refers to differences in $\delta^{18}O$ values that can occur in a particular storm event due to the duration and intensity of rainfall; light rainfall or rain from the early part of the storm may be enriched because of evaporation during the early part of its descent, whereas during larger storms with intense rainfall, the air below the cloud base may be more saturated, decreasing enrichment (Ingraham 1998). This effect is likely to be less at MORA compared with drier environments because falling snow is seldom subject to isotopic fractionation by exchange or evaporation.

Climate-driven fractionation events on the ground surface also drive variability in the isotope signal; potential phase changes in the snowpack, ice lenses and surface water, including isotope depletion caused by refreezing during cold periods and isotope enrichment occurring during snowmelt and ice melt during the spring thaw(s) are all integrated in the study basin $\delta^{18}O$ values. Assessments of variability such as the spatial and temporal changes in the 'amount effect' in precipitation and relative differences in ground surface fractionation processes between basins required fine-scale spatial and temporal $\delta^{18}O$ data that did not exist for this region.

Other studies have shown the importance of mixing processes within forested hillslopes associated with source waters released at different times from shallow groundwater and subsurface flow systems into the channel. Rainfall acts to displace 'old' waters from hillslope aquifers into the channel network. Stable isotope concentrations provide one method to synthesize this information on both subsurface and surface flowpaths from multiple sources (Maloszewski *et al*., 1992; Vitvar *et al*., 2002). Research comparing $\delta^{18}O$ values produced by precipitation from individual storms with concurrent measurements taken from channel discharge show that more than 50% of streamflow represented pre-event water, regardless of the sharp rises in streamflow that accompany major storm events (McDonnell, 2003; McGlynn *et al*., 2003; McGuire *et al*., 2005). However, although these mechanisms are certainly occurring in the forested hillslopes within the MORA study basins, in addition to $\delta^{18}O$ fractionation processes associated with atmospheric processes, these elements do not explain the differences in the MORA hydrological indices; all the basins are covered by forested hillslopes below subalpine elevations.

Like many hydrologic studies using stable isotopes, there was little previous research to compare with our data. Moreover, microclimate variability in these basins was such that detailed time series measurements of precipitation $\delta^{18}O$ values at one location in each basin did not adequately summarize the spatial extent of microclimate-scale differences among basins potentially reflected in an integrated isotope signal. Although it is inadvisable to rely solely on the stable isotope signal, the $\delta^{18}O$ values at the MORA sites proved useful when compared with streamflow patterns, water temperature and climate data.

### *Water temperature and the diurnal signal*

Water temperature time series and the amplitude of the diurnal signal were used to compare seasonal differences in hydrologic regimes among basins.

Alpine channels experience large annual ranges in air temperature and solar radiation; however, in groundwater-fed channels, water temperature is moderated by both the volume and temperature of groundwater inflows (Johnson, 2004). In cases where the proportion of groundwater influx is high, water temperature time series show virtually no variation in the diurnal signal and little annual variation in water temperature compared with surface runoff-dominated systems (Freeze, 1972; Constantz, 1998). Cooler water temperature regimes in summer (~5–7 °C) and warmer water temperatures in winter (~4 °C in North Cascades headwaters) are associated with streams that have a relatively large amount of groundwater discharge.

At the local scale, the effects of variations in stream temperature on the diurnal signal are affected by the infiltration rate imposed by the streambed surface (Constantz, 1998). For example, the heat capacity of a layer of fine-textured streambed material acts to thermally damp the magnitude of the diurnal variation in temperature as stream water percolates through the streambed. In the study headwaters, bedrock streambeds limit infiltration causing larger diurnal amplitudes, whereas streams flowing through coarse-grained colluvium have permeable gravel and sand streambeds that thermally moderate the temperature variation to such a degree that very little diurnal variation in streambed infiltration occurs.

The amplitude of the diurnal signal was measured by computing half the difference between the daily maximum and minimum water temperatures (Lundquist and Cayan, 2002). Continuous time series, using Onset Stowaway Tidbit Temperature Loggers (Onset Corp., N. Falmouth, MA, USA), were recorded from June through the end of August 2007 at each stream gage location within Lost,

Shaw, Crystal and Deer Creeks. Laughingwater Creek was omitted because of access problems resulting from a major flood in 2006. Because lower Shaw Creek flow was predominately subsurface at this location, a temperature logger was placed in the thalweg of a channel outlet just beyond the dry colluvial surface.

## RESULTS

### *Valley types*

Lost, Crystal and Shaw (LoCS) Creeks (Figure 4a–c) and Deer and Laughingwater (DLa) Creeks (Figure 5a–b) showed differences in the downstream configuration of valley types categorized along the channel longitudinal profile. Spatial patterns displayed by LoCS Creeks differed from those in DLa Creeks. Although all five basin profiles included alluvial and bedrock valley types, a greater proportion of LoCS channel length was identified as colluvial. Total source and sink colluvial channel length along Shaw, Crystal and Lost Creeks ranged 42–58%, whereas the DLa Creeks were 9–14%.

Source colluvial channels were found in subalpine upper headwaters, whereas sink colluvial channels occupied forested valleys and valley steps; both exhibited similar patterns in spatial extent along the channel profile, and both were typical of areas dominated by depositional talus and coarse debris from large mass movements (Figure 6a). LoCS source colluvial channels were found at 1600–1950 m in elevation, and sink colluvial channels were identified in an elevational zone of ~1000–1400 m. Source and sink colluvial channels areas were extremely limited in the DLa Creeks and followed no particular pattern along the elevational profile (Figure 6b).

Colluvial channels were linked to depositional landforms, such as talus slopes and relict rock glacier

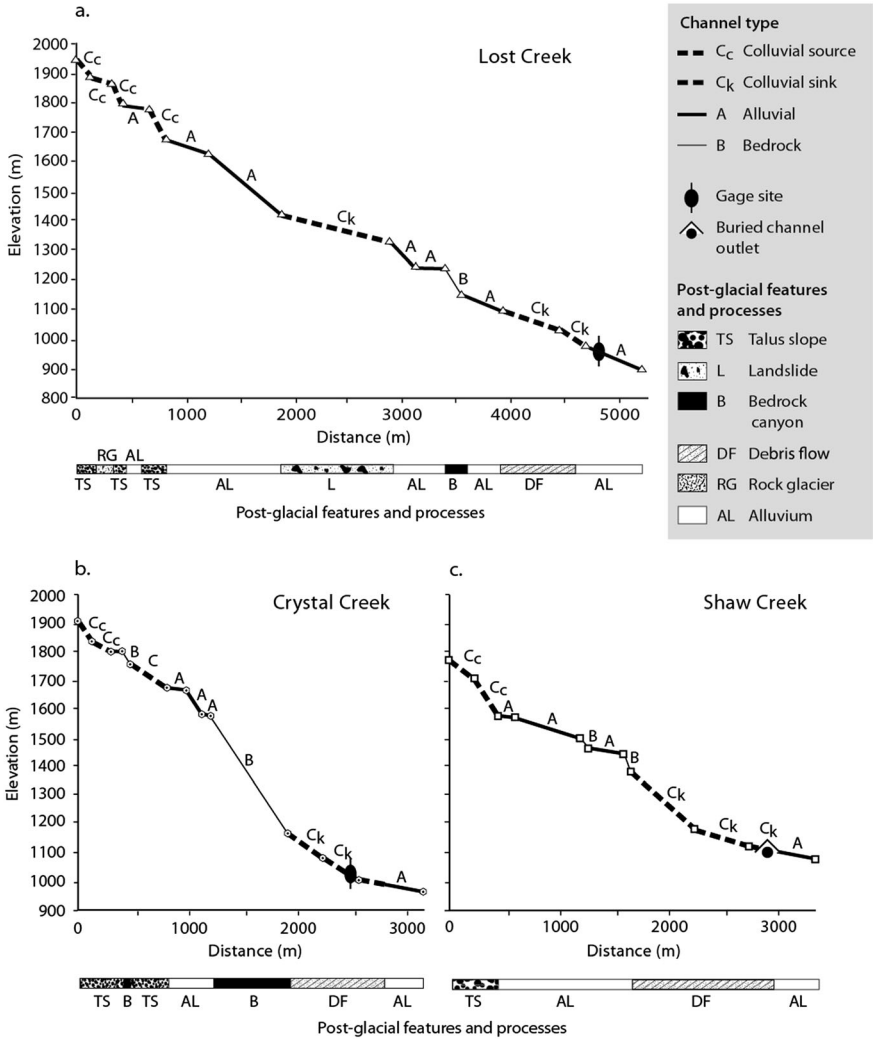


Figure 4. Longitudinal profiles for (a) Shaw, (b) Crystal and (c) Lost Creeks showing colluvial source, colluvial sink, alluvial and bedrock valley types and associated post-glacial features and landforms.

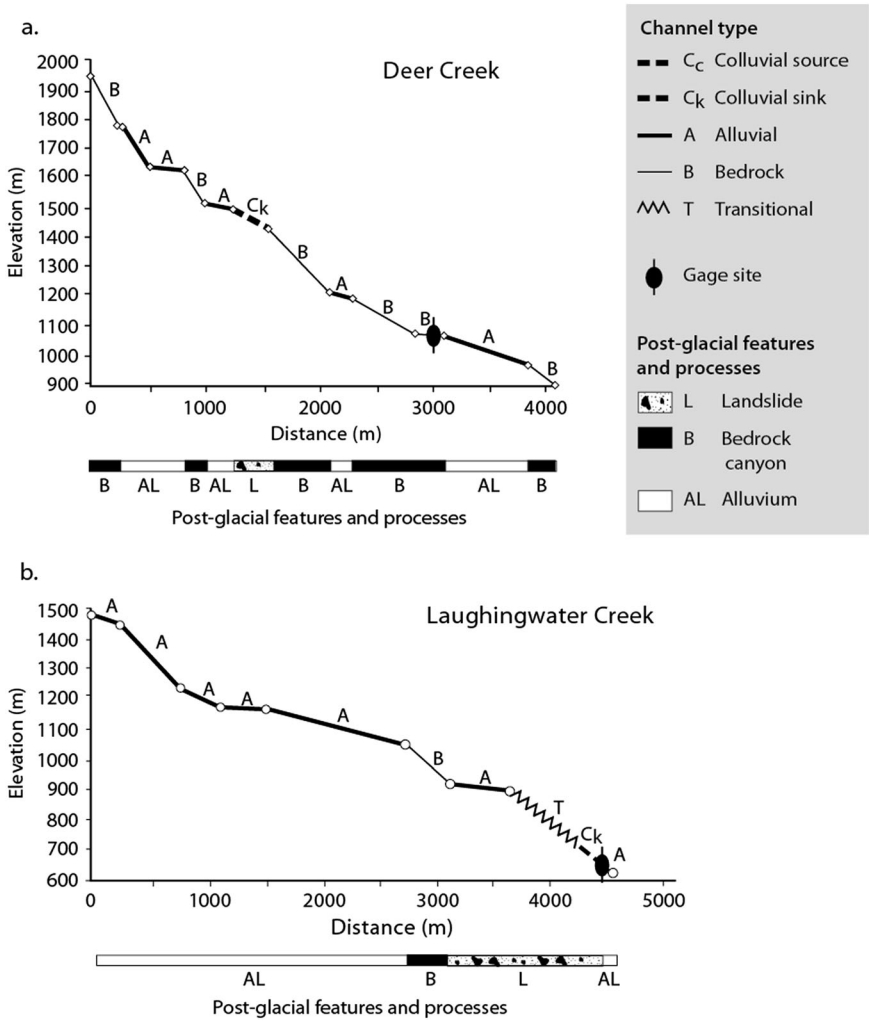


Figure 5. Longitudinal profiles for (a) Deer and (b) Laughingwater Creeks showing colluvial sink, alluvial and bedrock valley types and associated post-glacial features and landforms. Channel and valley morphology in the lower third of Laughingwater Creek is in transition due to a recent (1969) rotational landslide; a reach-scale landslide that occured during the November 2006 storm has altered the channel at the former gage site from an alluvial (cascade) to a sink colluvial type

deposits, with reversely sorted permeable fines (sands and small gravels) created by fluvial action found beneath the coarse-grained rock matrix. In cases where hydraulically sorted channel material was not visible, the sound of moving water was often audible beneath the rock mantle, deep within the depositional feature. These channels commonly alternated between subsurface and short daylighted surficial channel segments in contrast to alluvial channels that displayed typical fluvial processes and morphologies characteristic of mountain headwater channels (Montgomery and Buffington, 1997).

Sink colluvial channels flowed within colluvial landforms over great distances. For example, Lost Creek was buried in landslide debris for 1.2 km within a large hanging glacial valley. Shaw Creek's 1.3-km subsurface channel was buried by large debris flows that extended along the channel longitudinal profile; subsurface flow was continuous across valleys and valley steps (Figure 7). These channels lacked sufficient stream power to transport coarse debris; in addition, episodic debris flows did not erode through the deposited material or affect the antecedent stepped morphology of the longitudinal profile.

Not all sink colluvial channels at MORA can be easily differentiated from alluvial channels. Comparison of channel width, x-sectional area and discharge in segments with analogous drainage areas showed that the surficial expression of source and sink colluvial channels were undersized based on drainage area. When compared with larger lower-order channel segments found upstream, this incongruity provided an important diagnostic feature. For example, the sink colluvial portion of Crystal Creek was composed of what appeared to be an underfit alluvial channel flowing upon valley deposits. Discharge volume

 

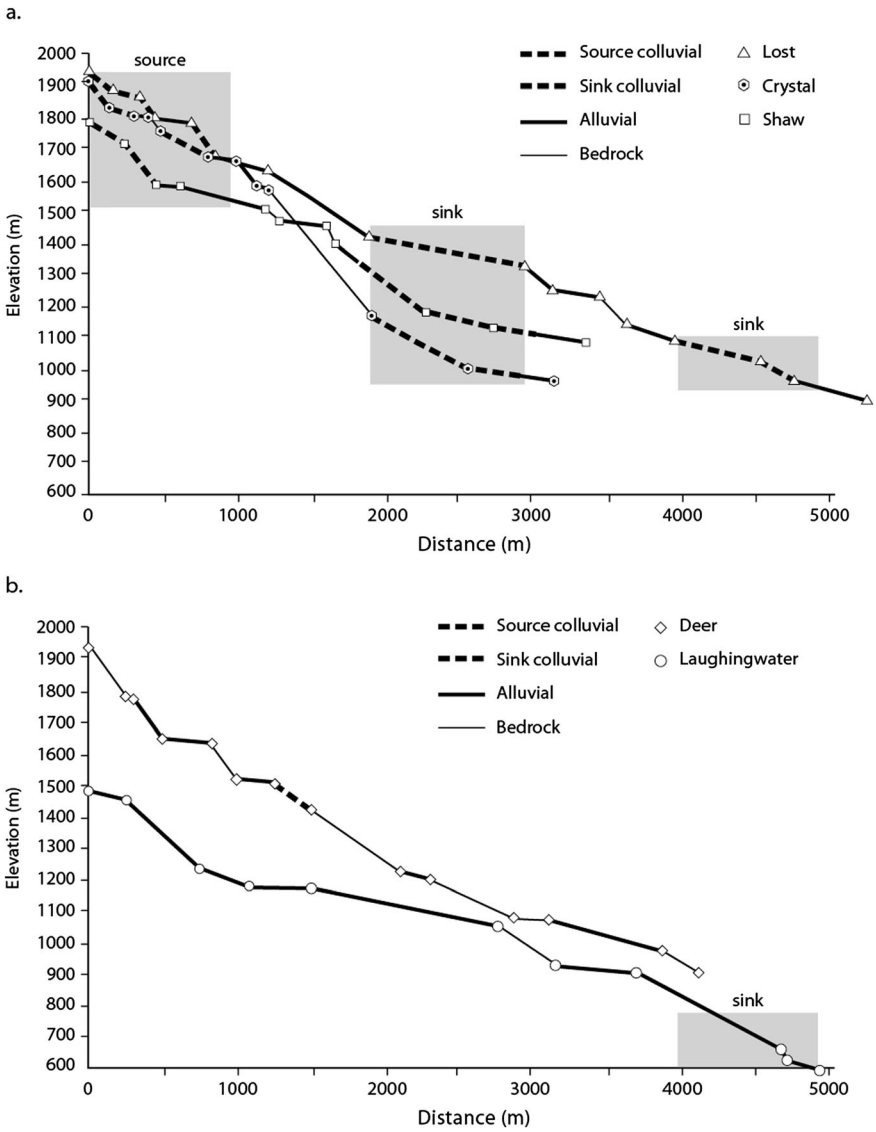


Figure 6. Longitudinal profiles of the LoCS Creeks (Lost, Crystal and Shaw) (a) illustrating similarities in the locations of the source and sink colluvial channel types along the stepped longitudinal profile produced by post-glacial mass wasting processes. In contrast, the DLa Creeks (Deer and Laughingwater) (b) do not exhibit the same geomorphic pattern. Shaded boxes, labelled as source and sink, define the elevational zones of colluvial channels

upstream was greater than discharge measured in the colluvial segment, because of multiple subsurface flowpaths.

### *Deer and Lost Creek: analogous metrics, differing seasonal hydrographs*

Deer and Lost Creeks were most alike of the five study basins in critical metrics such as drainage area (14.5 *vs* 14 $km^2$), gradient (11.3% *vs* 11%) and mean channel elevation (1456 *vs* 1423 m). Based on elevation, all basins were snow-dominated during the winter months, theoretically limiting basin-wide streamflows until late spring (Table I). However, comparison of seasonal streamflow hydrographs with water temperature time series and subregional scale climate data showed both anomalous fall and winter rain events and variation in response between the two basins in all conditions. For example, ARs and other winter rain and ROS events caused widespread runoff during the snow season, but these events did not overwhelm characteristic patterns of hydrologic response. Portions of Lost Creek flowed underneath the snow and rock mantle throughout much of the winter producing a steady winter baseflow discharge not present in Deer Creek. Differences in hydrologic response between Deer and Lost Creeks offered a useful comparison between colluvial and bedrock-dominated basins with few confounding factors such as differences in elevation and drainage area.

Figure 7. Shaw Creek was buried episodically by colluvium from hillslope debris flows that surge down-valley once they reach the main channel. However, surficial deposition has not altered the underlying stepped longitudinal profile. Streamflow beneath the coarse colluvial surface is audible in many locations

Lost Creek's peak flow volumes were consistently lower than those exhibited by Deer Creek, whose runoff dynamics reflect climate forcings (e.g. the magnitude and intensity of precipitation events and the snowmelt signal). In contrast, baseflow discharge volumes in Lost Creek exceeded those in Deer Creek during both cold winter and dry summer periods. For example, hydrograph comparison from late snowmelt to baseflow showed that Lost Creek's recession was very gradual compared with Deer Creek, characterized by multiple peak flows and a strong diurnal signal (Figure 8a). Deer Creek's runoff response more closely aligned with the steep declines in snow depths recorded from the Cayuse and Corral Pass SNOTEL stations. After snowmelt, the Lost and Deer Creeks discharge patterns were reversed; Lost Creek displayed a higher baseflow discharge than Deer Creek.

The larger subsurface and groundwater influx characteristic of colluvial channels affected Lost Creek's water temperature values during the same period (Figure 8b). During late snowmelt, Lost Creek's winter norm of 4 °C was the minimum of the narrow diurnal signal. In contrast, Deer Creek's minimum water temperature was just above 2 °C. Between 19/6/07 and 1/7/07, during the transition from snowmelt to baseflow, Deer Creek's water temperature values reversed, becoming higher than Lost Creek. Beyond this period, Lost Creek baseflow was cooler, with a moderated diurnal signal compared with Deer Creek, a consequence of greater groundwater influx during baseflow.

Exceptional storms also produced a similar pattern; a major AR occurred at Mount Rainier on 6–8 November 2006 causing widespread flooding and catastrophic debris flows. Between 20 and 46 cm of rain was recorded at different elevations in the park during the period of greatest precipitation. An unusually high freezing level (2440 m) occurred during the heaviest rainfall following 3 days of above-freezing air temperatures (Figure 9a). Antecedent moisture conditions caused by melting snow (25 cm at the Huckleberry SNOTEL station at ~714 m elevation) contributed to runoff.

The effects of these conditions on streamflow discharge (Figure 9b) paralleled differences in hydrologic regime between the two creeks produced by less intense rain and snowmelt events. The Deer Creek hydrograph did not begin to rise until 6/11/06 and Lost Creek rose 12 h later. However, both flood peaks occurred almost simultaneously. Deer Creek's discharge was >3× larger in volume during the storm although prior to and after the storm, flow volumes were reversed.

### *Hydrologic indices – recession constants*

The differences in hydrologic response between Lost Creek, with greater colluvial channel length, and Deer Creek were reflected in similar differences between Crystal and Laughingwater Creeks. Peak flows generated both during snowmelt and from fall and winter storms were consistently higher and baseflows lower in the DLa Creeks compared with the moderated peak flows and sustained baseflows exhibited by Crystal and Lost Creeks. Descriptive statistical analysis of computed recession constants ($K_r$) for the four gaged creeks (Lost, Crystal, Deer and Laughingwater) summarized from the entire period of record (2005–2007) confirmed these differences (Figure 10a). The higher median $K_r$ values for Crystal and Lost Creeks represented more gradual flow recessions, whereas the lower median values for DLa Creeks corresponded to higher peak flows and steeply falling recessions.

### *Hydrologic indices – stable isotopes*

Seasonal variations in $\delta^{18}O$ values among the basins using $\delta^{18}O$-based descriptive statistical analyses showed that the LoCS Creeks were more depleted in $\delta^{18}O$ than the DLa Creeks for all grab samples taken concurrently in the five creeks (Figure 10b). The variation in $\delta^{18}O$ patterns could not be explained by elevational, seasonal or 'amount effect' metrics given the similarities among the basins; the LoCS Creeks $\delta^{18}O$ values were depleted in all seasons compared with the DLa Creeks. Clustering of $\delta^{18}O$ results was similar to the differences in $K_r$ generated for the study basins (Figure 10a). Like the recession constants, the amount of variation of $\delta^{18}O$ values differed seasonally but maintained the same pattern in relation to each other.

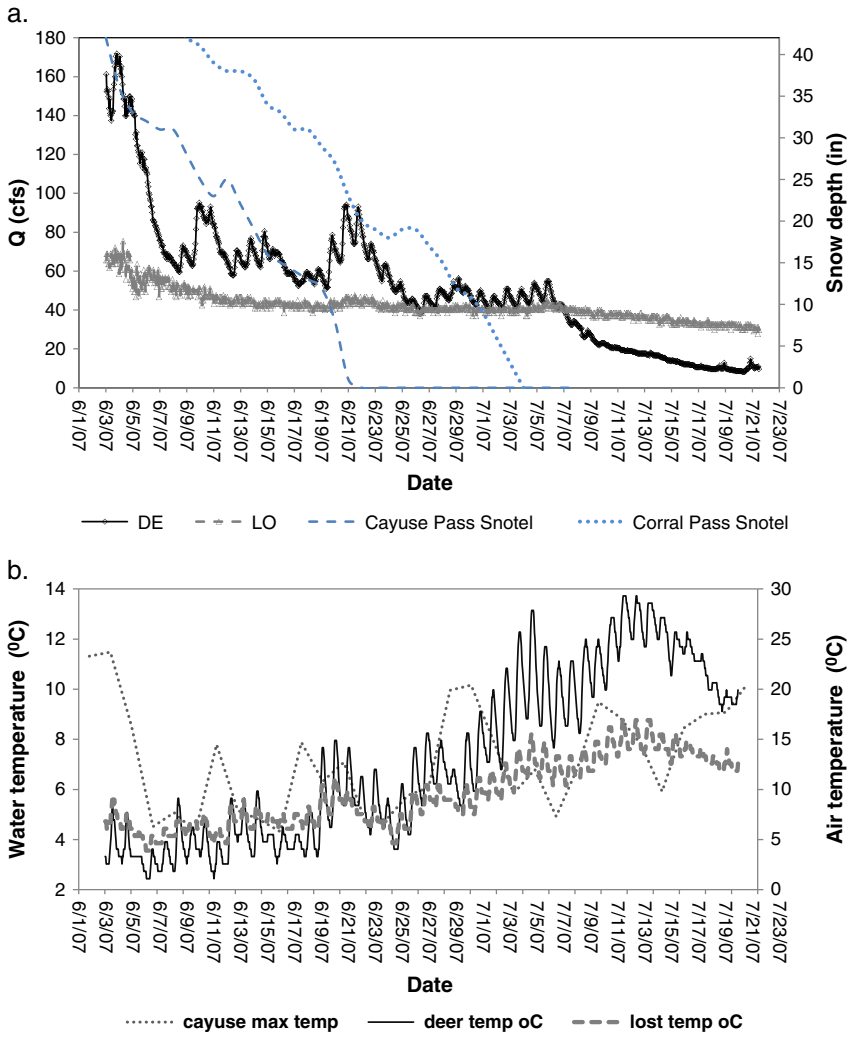


Figure 8. Comparison of (a) recession curve and snowdepth and (b) air and water temperature time series data occuring from late snowmelt to early baseflow (3/6–22/7/07) for Lost and Deer Creeks. (a) Snowdepths recorded at two SNOTEL stations, Cayuse Pass (dashed line) and Corral Pass (dotted line) are shown with recessions from Lost (thick continuous grey line with Δ symbol) and Deer (thin continuous black line with ◊ symbol) Creeks. The late spring recession for Deer Creek more closely reflects runoff generated by snowmelt; the falling limb for Lost Creek is much less pronounced. After snowmelt, baseflow volumes are greater in Lost than in Deer Creek. (b) Air temperature patterns (dotted line) are also more closely aligned with water temperatures in Deer Creek (thin continuous black line with ◊ symbol) after 19/6/07 than Lost Creek (thick continuous grey line with Δ symbol). Preceding 19/6/07, Deer Creek's minimum water temperature remained lower than Lost Creek, but the diurnal amplitude was consistently greater

We used Equation 1–3 (Burk and Stuiver, 1981) to compare the modelled 'elevation effect' by comparing the predicted $\delta^{18}O$ values generated from the equation using actual mean basin elevations with the observed median $\delta^{18}O$ values from the individual study basins (Figure 10b). Only the median $\delta^{18}O$ values for Deer Creek were analogous to the modelled values. The Laughingwater Creek modelled $\delta^{18}O$ values were also more enriched than those measured in the field.

Seasonal comparison of the 2006 dataset showed the most extreme differences between LoCS and DLa Creeks during baseflow (Figure 11a). Snowmelt values were the most depleted overall, whereas the DLa $\delta^{18}O$ values showed the greatest deviation from LoCS Creeks during baseflow. The $\delta^{18}O$ grab samples taken in the LoCS Creeks immediately after the 6 November 2006 storm were unusually enriched. While these unusually low values could not be compared with those from the DLa Creeks because of access issues, and AR of this magnitude is an outlier. As a result, runoff from intense rainfall dominated the isotope signal in the LoCS Creeks, producing the low $\delta^{18}O$ values.

### *Hydrologic indices – water temperature*

The lower range of water temperature values measured in Lost and Shaw Creeks (medians of 6.4 and 5.6 °C, respectively) matched $K_r$ and $\delta^{18}O$ values (Figure 10c).

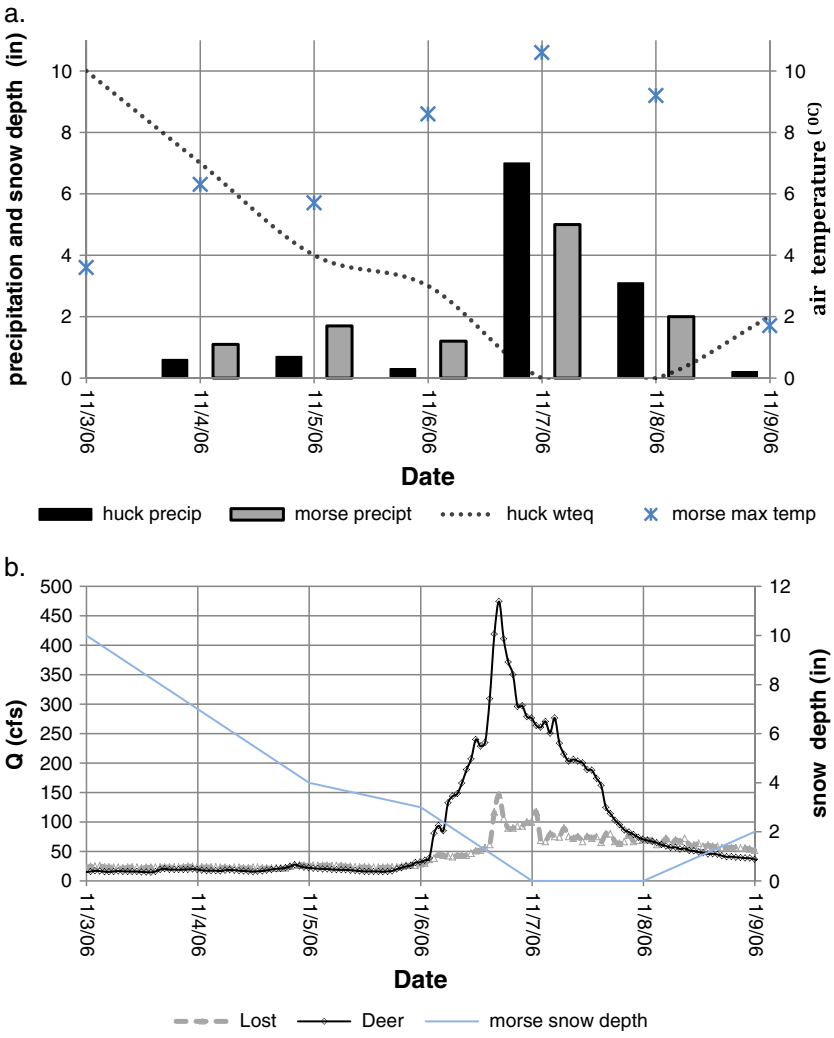


Figure 9. A major atmospheric river (AR) storm occurred 3–7 November 2006, producing intense rainfall and unusually high freezing levels. (a) Climate records indicated air above-freezing air temperatures recorded at 1850 m elevation (x), maximums of over 15 cm of rainfall 6 November 2006 (black column) recorded at 714 m elevation and 13 cm of rainfall at 1850 m (grey column) during a 12-h period the next day. Melting snow (dotted line) recorded at 714 m preceded the heaviest rain. (b.) Peak flows for Deer Creek (thin black line with ◊ symbol) were three times higher than Lost Creek (thick continuous grey line with Δ symbol) during the AR.

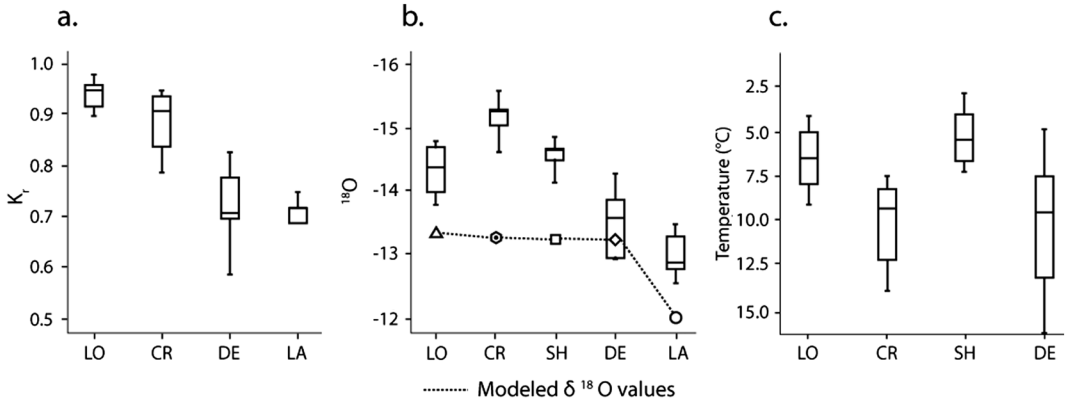


Figure 10. Boxplots of (a) $K_r$, (b) $\delta^{18}0$ and (c) water temperature between Lost (LO), Shaw (SH), Crystal (CR), Deer (DE), and Laughingwater (LA) Creeks. Box limits indicate 25th and 75th percentiles, and the dividing line indicates the median. Error bars show maximum and minimum values. Modelled $\delta^{18}0$ values using Buck and Stuiver (1981) are shown for comparison with measured values

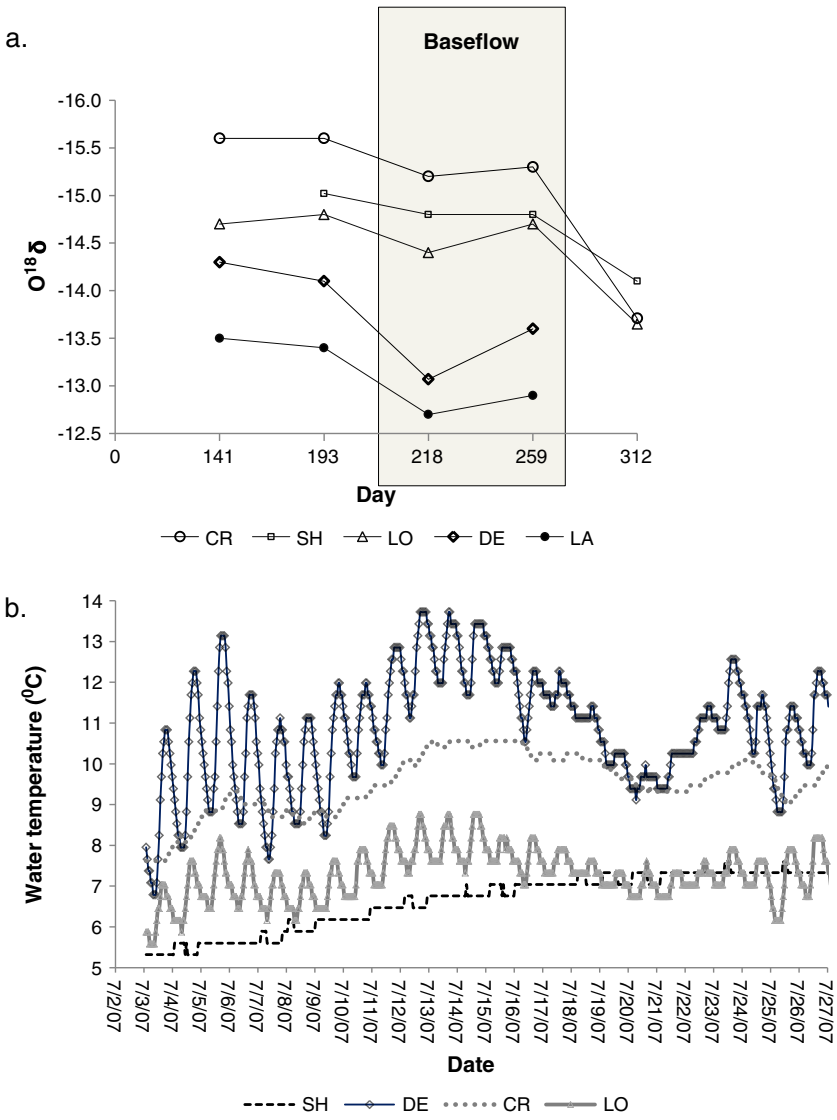


Figure 11. Comparison of (a) seasonal $\delta^{18}0$ patterns and (b) water temperature diurnal amplitudes among the study basins. The largest divergence in $\delta^{18}0$ signal between the LoCS and DLa Creeks is evident during baseflow (days 218 and 259). The LoCS Creek values shown for Day 312 were taken immediately after the November 2006 AR event; unseasonably warm and intense rainfall coming off the Pacific Ocean was responsible for the anomalous $\delta^{18}0$ values shown for the LoCS Creeks. Runoff from intense precipitation appears to have diluted the baseflow signal. The DLa Creeks were not sampled because of mass movements blocking all access. In contrast, (b) summer water temperature values and diurnal amplitudes at the end of snowmelt (3/7/07–27/7/07) during a period with no rain and intense solar radiation also highlight the variability of response among the basins. Deer Creek water temperature time series (thin black line with ◊ symbol) presented larger diurnal amplitudes especially at the end of snowmelt. Lost Creek (thick grey line with Δ symbol) showed a smaller diurnal signal with consistently lower water temperatures. Both Crystal (grey dashed line) and Shaw Creeks (black dashed line) lacked a distinct diurnal signal. However, the water temperature signal in Crystal Creek tracked the minimum values of the diurnal amplitudes of Deer Creek

Crystal Creek, with 6% greater mean slope and a smaller drainage area (i.e. lesser discharge than the other drainages) (Table I), showed water temperature values similar to the minimum temperature exhibited by Deer Creek. However, all channels with a higher proportion of colluvial channel length exhibited narrower diurnal temperature fluctuations, including Crystal Creek. Crystal and Shaw Creeks diurnal amplitudes did not exceed 0.5 °C, and Lost Creek was less than 0.8 °C (Figure 11b). In contrast, the Deer Creek diurnal amplitude exceeded 2 °C.

The similarity in water temperature between Deer and Crystal Creeks can be explained by the localized effects of solar radiation on surface water; Crystal Creek's steep bedrock canyon upstream of the gage site is over 1000 m in length, whereas Lost and Shaw Creeks have more extensive deep subsurface flowpaths. The heat capacity of water flowing through the coarse-grained porous subsurface is important as it acts to thermally damp water temperatures in Lost and Shaw Creeks. The relatively shallow colluvium at the Crystal Creek gage site was

sufficient to dampen the diurnal signal, while not adequate to cause sufficient heat loss to produce lower water temperatures.

*Depositional landforms as filters of hydrologic response*

Regression analyses comparing three hydrologic indices (median $K_r$, $\delta^{18}O$ and water temperature) with percent colluvial channel length along the longitudinal profiles showed differences between the LoCS Creeks (42–58% colluvial channel length) and the DLa Creeks (9–14% colluvial channel length) (Figure 12a–c). Lost and Shaw Creeks exhibited slow response $K_r$, depleted $\delta^{18}O$ values, moderated stream temperatures and lower diurnal amplitudes. Crystal Creek matched Lost and Shaw Creeks indices in all but summer water temperatures; whereas winter water temperatures remained close to 4 °C in all LoCS Creeks, during baseflow, Crystal Creek water temperatures followed the minimum daily values of the Deer Creek (Figure 12c). The DLa Creeks displayed consistently flashier response (i.e. lower) $K_r$ patterns, higher water temperatures with large amplitude diurnal signals during baseflow and more enriched and variable $\delta^{18}O$ values.

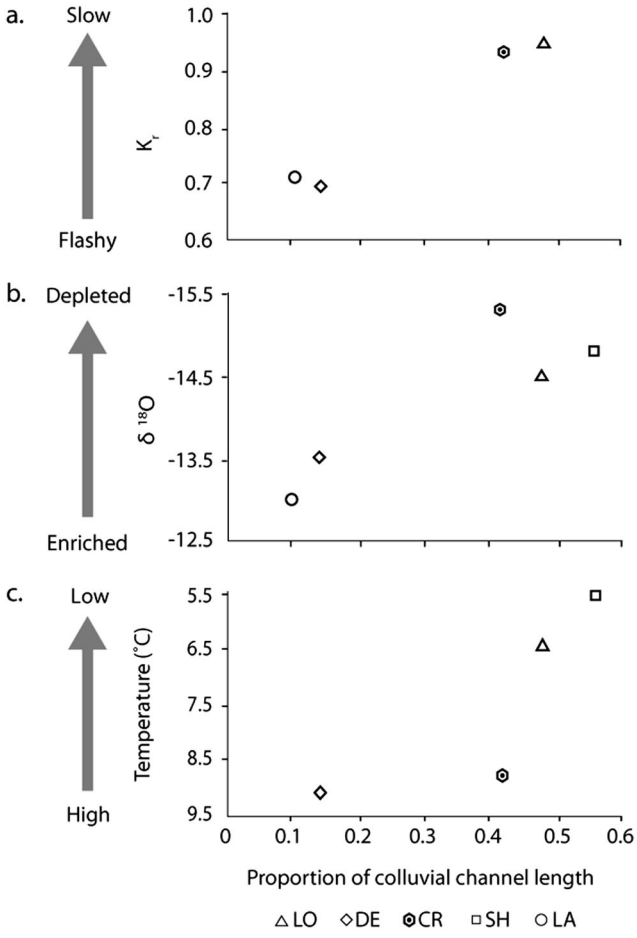


Figure 12. Proportion of colluvial channel length in Lost (LO), Shaw (SH), Crystal (CR), Deer (DE) and Laughingwater (LA) Creeks *versus* (a) median recession constant, (b) median $\delta^{18}0$ and (c) median water temperature. The *x*-axis for all basins is reversed to preserve basin groupings beginning with moderated flow characteristics associated with groundwater. The *y*-axis for water temperature is also reversed for the same reason

Median recession constants plotted against colluvial channel length showed a positive relationship, in which the high $K_r$ values found in Lost and Crystal Creeks were associated with greater colluvial channel length (Figure 12a). Shaw Creek, which had extensive sink colluvial channel length, also appeared to be a slow response system and displayed a depleted $\delta^{18}O$ signal and moderated water temperatures. In contrast, the lower $K_r$ values found in the DLa Creeks were negatively correlated with colluvial channel length.

Greater colluvial channel length also corresponded to a depleted $\delta^{18}O$ signal in the LoCS Creeks (Figure 12b). The DLa Creeks, which were comparatively enriched in $\delta^{18}O$, primarily exhibited bedrock and alluvial channel types (≥86%). Comparisons between median water temperature and percent colluvial area (Figure 11c) were consistent with the other interbasin relationships. Water temperature also followed the same pattern (Figure 12c).

## DISCUSSION

Accounting for the association between geomorphic landforms and hydrologic response in glaciated alpine headwaters provides a critical link between regional process controls (climate, geology and topography) and finer-scale hydrologic indices. Our approach categorized valley-scale channel types or process domains along the stepped channel longitudinal profile as a framework to characterize differences in streamflow response. Using this information, we evaluated the properties and effects of the proportion of colluvial channel length on hydrologic indices measured at the basin scale. This relationship, useful in the Cascade Mountains, could also provide insight in other temperate glaciated mountain ecosystems.

Results from the three hydrologic indices used in this study, in combination with our geomorphic assessment, suggest that colluvial channels and landforms have a marked effect on the complex suite of hydrological processes found in alpine headwaters. The $\delta^{18}O$ results corroborate the information provided by the recession constants and seasonal hydrographs. The moderated streamflows exhibited by the LoCS colluvial basins and more flashy hydrographs in the DLa Creeks (controlled by fluvial processes) reflect consistent patterns in hydrologic response and variation in median $\delta^{18}O$ values displayed by the LoCS and DLa Creeks. These patterns are not associated with differences in precipitation

regimes, seasonality, drainage basin area, aspect, elevation and slope but represent the effect of current and historic geomorphic processes on basin structure.

Seasonality in $\delta^{18}O$ precipitation values produces large variations in the isotope signal; for example, a ~6.6‰ difference was recorded in spring to summer precipitation values at Cle Elum, WA, in 2006 (Ingraham, 1998, Robertson and Gazis, 2006). In contrast, $\delta^{18}O$ values in streamflow discharge sampled in the study basins during snowmelt (May), late spring melt (July) and late summer (August and September) showed less variation than variation in the precipitation signal at Cle Elum.

The 'altitude effect', considered the second most important cause of variability in the $\delta^{18}O$ precipitation signal (Ingraham, 1998), also did not correspond to measured discharge $\delta^{18}O$ values; median LoCS streamflow $\delta^{18}O$ values were more depleted than (modelled) precipitation values in spite of the similarity in elevation between basins. Isotope fractionation processes occurring on the ground surface, such as enrichment of $\delta^{18}O$ values during snowmelt, were also not evident as a distinct isotope signal among the basins.

The differences in median $\delta^{18}O$ concentrations and seasonal patterns in hydrologic response among the basins correspond to the spatial extent of depositional landforms and associated colluvial channel morphologies. Relatively little is known about the hydrologic characteristics of upper basin features such as talus slopes and rock glacier deposits coupled with the dynamics of colluvial channels flowing through large-scale mass movement debris (Millar and Westfall, 2008). However, research has shown that the coarse-grained surficial deposits common to such features store recharge waters as groundwater and interstitial ice (Lui *et al*., 2004; Roy and Hayashi, 2009). The slow recession and higher baseflows associated with snowmelt in Lost Creek compared with Deer Creek support these findings (Figure 8a); the gradual decline of the falling limb in the Lost Creek hydrograph may be due to the contribution of interstitial ice melt throughout the summer months augmented by the release of groundwater stored in sand lenses below the rock mantle. For example, within the Lost Creek basin, yearly observations of an unusually rapid decline in Upper Palisades Lake water levels after snowmelt may be caused by ice within the talus matrix damming the lake until the interstitial ice has melted. This scenario suggests melting of subsurface ice requires a longer period of warm weather, contributing to differences in channel response in basins with colluvial landforms.

The timing of streamflows caused by melting ice within coarse-grained features appears to be delayed, occurring after snowmelt has ceased. Subsurface flows associated with colluvial post-glacial features, filtering slowly through fine-grained underlying sediments, would also be associated with a slow response, producing a relatively large source of baseflow (Clow *et al*., 2003). Sink colluvial channels constrained within narrow glacial valleys and troughs overlain by mass wasting debris may support groundwater storage; buried channels may also funnel flow through colluvium. However, the full range of mechanisms is unknown and could vary widely across the landscape.

Landscape organization is a first-order control on both the mean residence time of catchment waters and the streamflow regimes associated with storage and filtering mechanisms (McGlynn *et al*., 2003). We found that the $\delta^{18}O$ isotope signal from colluvial channels flowing through depositional structures affected discharge values through the following mechanisms: (1) water storage and mixing processes within upper basin depositional landforms associated with exfiltration in headwater channel initiation zones that also act to delay delivery of large quantities of seasonally depleted $\delta^{18}O$, (2) delay of the delivery of depleted $\delta^{18}O$ due to buffering of direct climate impacts (i.e. solar radiation and air temperatures at the ground surface) by the coarse-grained rock mantle associated with both colluvial landforms and channels, (3) buffering of source waters from fractionation associated with additional phase changes occurring on the land surface and (4) storage and mixing processes that also delay delivery of the seasonally depleted $\delta^{18}O$ signal within channel sinks after streamflow infiltrates into glacial valley colluvium. In the case of sink colluvial channels, upstream flows from alluvial or bedrock channels with high stream power are funnelled directly into large sediment-filled colluvial sinks (e.g. Lost and Shaw Creeks). As all or a portion of the discharge infiltrates into deeper subsurface flowpaths and buried channels, streamflow may be routed into shallow aquifers while previously stored waters are released.

The $\delta^{18}O$ concentrations in the LoCS Creeks may be best explained by the delayed routing of recharge with a depleted $\delta^{18}O$ signal from winter storms at high elevations. Similar effects have been shown in other mountain environments where discharge from groundwater-fed mountain springs with longer transit times is more depleted in $\delta^{18}O$ than surface channels in the same region due to a higher percentage of winter/high elevation recharge in the summer months (Rice, 2006). In the LoCS Creeks, these recharge waters are stored and released from within the permeable, finer-grained sediments underlying colluvial features and channels. In the upper basins, they are mixed with meltwater from ephemeral ice lenses within talus slopes and relict rock glacier deposits. Subsequent runoff helps to move these waters downstream.

Median water temperature patterns and percent colluvial area were generally consistent with the other interbasin relationships, with the exception of water

temperatures measured at the gage location on Crystal Creek. The apparent anomaly between the colluvial characteristics associated with $K_r$ and $\delta^{18}0$-derived metrics and water temperature patterns found in Crystal Creek appears to be caused by the localized nature of water temperature measurements. In small headwater channels, water temperature reflected localized effects from upstream solar radiation, shading and other metrics (Johnson, 2000; 2004) in contrast to $K_r$ and $\delta^{18}O$, which are assumed to integrate basin-wide characteristics (Vitvar *et al.*, 2002). In lower Crystal Creek, discharge from a bedrock channel segment flows into an undersized surface channel underlain by colluvium. We suspect that exchange processes associated with comparatively short, shallow flowpaths connected to the surficial channel did not have sufficient volume locally to cool stream temperatures at the gage site. In contrast, extensive sink colluvial channels, such as the $\geq$1 km length of buried channel lower Lost and Shaw Creeks, had a pronounced effect on downstream water temperatures in the channel. Variation between LoCS and DLa Creeks reflected differences in internal storage, filtering and routing mechanisms between basins.

Additional research is needed to better differentiate between processes associated with post-glacial structures (Roy and Hayashi, 2009). Critical components of fine-scale hydrologic features within relict rock-mantled landforms, especially groundwater occurrence and internal processes, are difficult to measure without specialized hydrologic tools that are not designed for the coarse-grained deposits found in these systems (Clow *et al.*, 2003). Even when instrumentation is feasible, modelling applications that require temporally continuous hydrologic data within spatially continuous models of the land surface (LiDAR) may not be easily accomplished in these complex topographies. Grid-based representations of climate, topography, vegetation, soil moisture content and other hydrologic drivers are not easily adapted to the heterogeneous spatial patterns that structure stream basins (Woods, 2002). The usefulness of hydrologic time series, which is necessary for understanding ecologically important temporal patterns, is dependent on the skill with which such measurements are deployed in order to characterize spatial complexity. Our study results suggest that key features of the hydrograph, such as rate of recession and temperature variability, are correlated with more easily surveyed geomorphic variables.

## CONCLUSION

We found that recession constants, water temperature and $\delta^{18}O$ stable isotope analyses were correlated with the extent of colluvial features found along channel longitudinal profiles in five MORA headwater basins. All study catchments exhibited valley-scale landform structures produced by mass wasting processes in the context of a paraglacial landscape, but streamflow regimes were associated with differences in the distribution and extent of colluvial and fluvial process domains that accounted for streamflow variability between basins. In particular, colluvial features and landforms were a good indicator of slow response hydrologic characteristics such as moderated streamflow and water temperatures regimes.

Interconnections between geomorphic controls and hydrologic response in glaciated mountain headwaters are difficult to assess without the benefit of an intermediate-scale spatial context. Ultimately, the morphology of these structures and their associated processes provide context for habitat-scale hydrologic and ecosystem variables (e.g. streamflow, water temperature and substrate) and landscape-scale disturbance processes and stressors (e.g. climate) necessary for understanding ecosystem function. Information provided by small-scale channel variables is limited by the spatial heterogeneity and complex temporal dynamics that control alpine basins. Identifying associations between process and morphology at different spatial and temporal scales is important for characterizing spatial variation of hydrologic response in a geomorphic context.

The ability to connect the functional components of paraglacial landforms with hydrologic characteristics across scales is necessary to develop process-based models in glaciated mountain headwaters. By differentiating between the valley-scale structural components that filter atmospheric recharge waters, it will be possible to identify the causal mechanisms that drive these ecosystems and better detect and mitigate the effects of ecosystem change.

### ACKNOWLEDGEMENTS

This work was funded by the National Park Service Natural Resource Preservation Program in conjunction with the US Geological Survey. Additional support was provided by the National Park Service North Coast and Cascades Network, North Cascades National Park and Mount Rainier National Park. Earlier versions of the manuscript were greatly improved by comments from P. Kennard, J. O'Connor and J. Riedel. Any use of trade, product or firm names is for descriptive purposes only and does not imply endorsement by the US Government.

### REFERENCES

Brardinoni F, Hassan MA. 2006. Glacial erosion, evolution of river long profiles, and the organization of process domains in mountain drainage

 

basins of coastal British Columbia. *Journal of Geophysical Research* **111**(F01013). doi: 10.1029/2005JF000358.

Brardinoni F, Hassan MA. 2007. Glacially induced organization of channel-reach morphology in mountain streams. *Journal of Geophysical Research* **112**(F03013). doi: 10.1029/2006JF000741.

Brown LE, Hannah DM, Milner AM. 2003. Alpine stream habitat classification: an alternative approach incorporating the role of dynamic water source contributions. *Arctic Antarctic and Alpine Research* **35**: 313–322.

Brown LE, Hannah DM, Milner AM, Soulsby C, Hodson A, Brewer MJ. 2006. Water source dynamics in an alpine glacierized river basin (Taillon-Gabietous, French Pyranees). *Water Resources Research* **42**: W08404.

Brown LE, Hannah DM, Milner AM. 2007. Vulnerability of alpine stream biodiversity to shrinking glaciers and snowpacks. *Global Change Biology* **13**: 958–966.

Brown LE, Hannah DM, Milner AM. 2009. ARISE: a classification tool for Alpine River and Stream Ecosystems. *Freshwater Biology* **54**: 1357–1369.

Burk RL, Stuiver M. 1981. Oxygen isotope ratios in trees reflect mean annual temperature and humidity. *Science* **211**: 1417–1419.

Clow DW, Schrott L, Webb R, Campbell DH, Torizzon A, Dornblaser M. 2003. Groundwater occurence and contributions to streamflow in an alpine catchment, Colorado Front Range. *Ground Water* **41**: 937–950. Press: Seattle; 79–128.

Collins BD, Montgomery DR. 2011. The legacy of Pleistocene glaciation and the organization of alluvial process domains in the Puget Sound region. *Geomorphology* **126**: 174–185.

Constantz J. 1998. Interaction between steam temperature, streamflow, and groundwater exchanges in alpine streams. *Water Resources Research* **34**: 1609–1615.

Crandell DR. 1969. Surficial Geology of Mount Rainier National Park, Washington. U.S Geological Survey.

Criss RE. 1999. *Principles of Stable Isotope Distribution*. Oxford University Press: Oxford.

Dansgaard W. 1964. Stable isotopes in precipitation. *Tellus* **16**: 436–468.

Downes BJ. 2010. Back to the future: little-used tools and principles of scientific inference can help disentangle effects of multiple stressors on freshwater ecosystems. *Freshwater Biology* **55**(Supplement 1): 60–79.

Fetter CW. 2001. *Applied Hydrogeology*, 4th ed. Prentice-Hall: Upper Saddle River, New Jersey.

Freeze RA. 1972. Role of subsurface flow in generating surface runoff: baseflow contributions to channel flow. *Water Resources Research* **8**: 609–623.

Frissell CA, Liss WJ, Warren CE, Hurley MD. 1986. A hierarchical framework for stream habitat classification: viewing streams in a watershed context. *Environmental Management* **10**: 199–214.

Grant GE, Swanson FJ, Wolman MG. 1990. Pattern and origin of stepped-bed morphology in high-gradient streams, Western Cascades, Oregon. *Bulletin of the Geological Society of America* **102**: 340–352.

Ingraham NL. 1998. Isotope variation in precipitation, chapter 3. In *Isotope Tracers in Catchment Hydrology*, Kendall C, McDonnell JJ (eds.). Elsevier: Amsterdam, The Netherlands; 87–118.

Johnson SL. 2000. Stream temperature response to forest harvest and debris flows in western Cascades, Oregon. *Canadian Journal of Fisheries and Aquatic Sciences* **57**(Supplement 2): 30–39.

Johnson SL. 2004. Factors influencing stream temperatures in small streams: substrate effects and a shading experiment. *Canadian Journal of Fisheries and Aquatic Sciences* **61**: 913–923.

Klemes V. 1988. A hydrological perspective. *Journal of Hydrology* **100**: 3–28.

Lui F, Williams M, Caine N. 2004. Source waters and flow paths in an alpine catchment, Colorado Front Range, United States. *Water Resources Research* **40**(W09401). doi: 10.1029/2004WR003076.

Lundquist J, Cayan DR. 2002. Seasonal patterns in diurnal cycles in streamflow in the Western United States. *Journal of Hydrometeorology* **3**: 591–603.

Maloszewski P, Rauert W, Trimborn P, Herrmann A, Rau R. 1992. Isotope hydrological study of mean transit times in an alpine basin (Wimbachtal, Germany). *Journal of Hydrology* **140**: 343–360.

McDonnell JJ. 2003. Where does water go when it rains? Moving beyond the variable source area concept of rainfall-runoff response. *Hydrological Processes* **17**: 1869–1875.

McDonnell JJ, Sivapalan M, Vache K, Dunn S, Grant G, Haggerty R, Hinz C, Hooper R, Kirchner J, Roderick ML, Selker J, Weiler M. 2007. Moving beyond heterogeneity and process complexity: a new vision for watershed hydrology. *Water Resources Research* **43**: 1–6.

McGlynn B, McDonnell J, Stewart M, Seibert J. 2003. On the relationship between catchment scale and stream water mean residence time. *Hydrological Processes* **17**: 175–181.

McGuire KJ, McDonnell J, Weiler M, Kendall C, Welker J, McGlynn B, Seibert J. 2005. The role of topography on catchment-scale water residence time. *Water Resources Research* **41**(WO5002). doi: 10.1029/2004WR003657.

Millar CI, Westfall RD. 2008. Rock glaciers and related perglacial landforms in the Sierra Nevada, CA, USA; inventory, distribution, and climatic relationships. *Quaternary International* **188**: 90–104.

Milner AM, Petts GE. 1994. Glacial rivers: physical habitat and ecology. *Freshwater Biology* **32**: 295–307.

Montgomery DR, Buffington JM. 1997. Channel-reach morphology in mountain drainage basins. *Geological Society of America Bulletin* **109**: 596–611.

Montgomery DR. 1999. Process domains and the river continuum. *Journal of the American Water Resources Association* **35**: 397–410.

Montgomery DR, Dietrich WE. 2002. Runoff generation in a steep, soil-mantled landscape. *Water Resources Research* **38**(9): 1–8.

Neiman PJ, Schick LJ, Ralph, FM, Hughes, M, Wick GA. 2011. Flooding in Western Washington: the connection to atmospheric rivers. *Journal of Hydrometeorology* doi:10.1175/2011JHM1358.1.

Poff NL. 1997. Landscape filters and species traits: towards mechanistic understanding and prediction in stream ecology. *Journal of the North American Benthological Society* **16**: 391–409.

Ralph FM, Dettinger MD. 2011. Storms, floods, and the science of atmospheric rivers. *EOS, Transactions American Geophysical Union* **92**: 265–272.

Rantz SE. 1982. Measurement and computation of streamflow: volume 1. Measurement of Stage and Discharge, Geological Survey Water-Supply Paper 2175: 284.

Rice SE. 2006. Level 2 springs inventory of the escalante river headwaters area, Grand Staircase-Escalante National Monument. Bureau of Land Management Cooperative Agreement No. JSA041002.

Robertson J, Gazis C. 2006. An oxygen isotope study of seasonal trends in soil water fluxes at two sites along a climate gradient in Washington State (USA). *Journal of Hydrology* **328**: 375–387.

Rodhe A. 1998. Snowmelt-dominated systems, chapter 12. In *Isotope Tracers in Catchment Hydrology* Kendall C, McDonnell JJ (eds.). Elsevier: Amsterdam, The Netherlands; 391–434.

Roy JW, Hayashi M. 2009. Multiple, distinct groundwater flow systems of a single moraine – talus feature in an alpine watershed. *Journal of Hydrology* **373**: 139–150.

Swanson FJ, Kratzy TK, Caine N, Woodmansee RG. 1988. Landform effects on ecosystem patterns and processes. *Bioscience* **38**: 92–98.

Tallaksen LM. 1995. A review of baseflow recession analysis. *Journal of Hydrology* **165**: 349–370.

Tsukada, M, Sugita, S, and Hibbert, DM. 1981. Paleoecology in the PNW: late quaternary vegetation and climate. *Verhandlungen der Internationalen Vereinigung für Theoretische und Angewandte Limnologie* **21**: 730–737.

Vitvar T, Burns DA, Lawrence GB, McDonnell JJ, Wolock DM. 2002. Estimation of baseflow residence times in watersheds from the runoff hydrograph recession: method and application in the Neversind watershed, Catskill Mountains, New York. *Hydrological Processes* **16**: 1871–1877.

Ward JV. 1994. Ecology of alpine streams. *Freshwater Biology* **32**: 277–294.

Weekes A, Torgersen C, Montgomery DR, Woodward A, Bolton SR. 2012. A process-based hierarchical framework for monitoring glaciated mountain headwaters. *Environmental Management* **50**: 983–997.

Wolock DM, Fan J, Lawrence B. 1997. Effects of basin size on low-flow stream chemistry and subsurface contact time in the Neversink River Watershed, New York. *Hydrological Processes* **11**: 1273–1286.

Woods R. 2002. Seeing catchments with new eyes. *Hydrological Processes* **16**: 1111–1113.

 